A Deep Learning Approach for Short-Term Solar Irradiance Forecasting using Maximal Overlap Discrete Wavelet Packet Transform and Hybrid CNN-LSTM-MLP Networks

Zahiir Coya[1, a)], Abdel Khoodaruth[1], Harry Ramenah[2], Vishwamitra Oree[3], Anshu Prakash Murdan[3] and Camel Tanougast[2]

[1]*Mechanical and Production Engineering Department, University of Mauritius.*
[2]*LGIPM, Université de Lorraine, Metz, France.*
[3]*Department of Electrical and Electronic Engineering, University of Mauritius.*

[a)] *Corresponding author: muhammad.coya2@umail.uom.ac.mu*

Abstract. The intermittency of solar energy poses threats to the integration of photovoltaic (PV) systems into the power grid. This necessitates highly accurate short-term forecasting models to stabilize and secure grid operation. This paper introduces a novel hierarchical model combining Maximal Overlap Discrete Wavelet Packet Transform (MODWPT) with a hybrid 1D-CNN-LSTM-MLP network for 15-minute-ahead solar irradiance forecasting. The MODWPT decomposes the original time-series into eight sub-series, which are then processed by a 1D-Convolutional Neural Network (CNN) to extracts local, high-frequency features, a Long Short-Term Memory (LSTM) network then captures temporal dependencies, and finally a Multi-Layer Perceptron (MLP) performs the final non-linear regression. The proposed model is evaluated against two hybrid deep learning models namely, MODWPT-LSTM-MLP and MODWPT-LSTM using a two-year dataset from Mauritius. The proposed model achieves a superior performance with MAE of 5.95, RMSE of 7.75, and MBE of -1.66. A detailed hourly analysis confirms its robustness during forenoon and afternoon periods, demonstrating that hierarchical feature extraction is essential for accurate solar forecasting.

Keywords: Solar Irradiance; Forecasting; Wavelet Transform; Deep Learning.

INTRODUCTION

Over the years, the rising oil prices, the ongoing depletion of fossil fuels, and mounting environmental concerns have significantly increased the use of PV power systems. Nevertheless, the intermittent character of solar energy threatens the stability, reliability, operational planning, and economic advantages of the electric grid [1]. Therefore, predicting PV power output and end-user demand are essential for foreseeing the demand from end-users and optimize the utilization of available energy resources [2]. Forecasting methods allow the management of the intermittent nature of solar energy and facilitates the integration of PV system into power grids.

Forecasting methods are commonly divided into two categories. The direct forecasting approach which predict PV power directly. In contrast, the indirect forecasting methods focus on the forecasting of solar irradiance. With data privacy policies limiting access to historical PV data of solar energy firms, solar irradiance prediction appears more attractive [3]. Models that predict solar irradiance can be classified into four main categories namely empirical approaches, models based on imagery, statistical models, and Artificial intelligence (AI) techniques.

Empirical models employ meteorological and geographical data to forecast Global Horizontal Irradiance (GHI), resulting in temperature-based, cloudiness based, sunshine-based, and hybrid models. In general, empirical models generally do not require a large amount of historical data, however, their accuracy depends on the availability of weather forecast data [4], and high computational costs with limited applicability for short-term GHI forecasts [5].

Image-Based models employ sky camera or satellite images to forecast GHI and are highly effective for large area predictions [6]. Their high temporal and spatial resolution provide important information on the movement of clouds.

However, limited image availability, high costs for imaging equipment, and the complexity of image processing reduce the widespread adoption of satellite image-based GHI prediction [7]. Statistical methods try to establish mathematical relationships based on predictors to forecast future values. However, non-stationarities in solar irradiance data caused by factors like cloud cover and seasonal variation can reduce the accuracy of these models in capturing nonlinear trends [8]. Some statistical methods include ARMA, ARIMA, exponential smoothing and even the Johansen VECM model as presented in [9] which deal with non-stationarity and causality properties.

Artificial intelligence techniques such as Machine Learning (ML) and Deep Learning (DL) models are extensively used in solar irradiance prediction and often outperformed the statistical approaches and physical methods [10]. Nonetheless, ML models are limited due to their dependence on personal experience and prior knowledge on the problem [11], their limited generalization capabilities [12] and their instability, high computational cost, and non-convergence of parameters when handling large data set with complicated and high dimensional data [13]. On the other hand, DL models demonstrate strengths in three main areas, namely automatic feature extraction with little or no underlying knowledge and expertise, robust generalization capability, and ability to deal with a large training dataset [14]. This has prompted researchers to shift their focus more on DL architectures. For instance, study [15] highlight the growing reliance on hybrid DL approaches, particularly those combining data preprocessing techniques with DL models.

In this context, the current study developed a hybrid method grounded on the coupling of wavelet packet transform (WPT) and several DL algorithms for the short term solar irradiance forecasting. Maximal overlap discrete wavelet packet transform (MODWPT) is employed to decompose the irradiance time-series into multiple subseries which are then fed into different networks comprising of 1D Convolutional Neural Network (CNN), Long Short-Term Memory (LSTM) and multi-layer perceptron (MLP). The outputs are then reconstructed to furnish the final 15 minutes ahead solar irradiance prediction. This study compares the forecasting performance of three hybrid models namely the MODWPT-CNN-LSTM-MLP, MODWPT-LSTM-MLP and the MODWPT-LSTM detailed in section 3.

The next section describes the tools employed for data gathering and cleaning. Section 3 elaborates on the proposed forecasting models. Section 4 details the performance metric employed in this study. In Section 5, the forecasts of each models are compared and discussed using relevant metrics and plots. Finally, concluding comments are given in Section 6.

DATA GATHERING AND CLEANING

The experimental setup comprises of a 20 kWp grid-tied PV system found on the roof of the University of Mauritius Library, with coordinates 20° 14' 6" S and 57° 29' 49" E. The PV panels are installed on a stationary frame that is inclined at 20 degrees and faces north. A thermopile SMP3 pyranometer with a spectral range of 300 to 2800nm is set up on the mounting structure to measure incident solar irradiance, while a PT100 sensor with a temperature range of -50 to 100°C measures PV module temperature. The structure also includes a WS600 allin-one weather sensor that measures ambient air temperature, the direction and speed of wind, relative humidity, and air pressure. All measured data is stored to the internal memory of a GL240 data logger and meets EN 61326-1 Class A specifications. The dataset spans over more than two years, beginning in July 2019 and ending in September 2021. The recorded data is filtered to exclude missing data and data collected between 4:30 p.m and 7:30 a.m were disregarded.

THE PROPOSED FORECASTING FRAMEWORKS

This study proposes three forecasting frameworks namely the MODWPT-CNN-LSTM-MLP, MODWPT-LSTM-MLP and the MODWPT-LSTM. All models employ LSTM, implying its necessity for modeling time dependencies.

The framework of MODWPT-CNN-LSTM-MLP is detailed as follows. The current study employs only GHI time series data. 80% of the total dataset was employed for training and the testing data comprises of 20% remaining data. The solar irradiance data is split into eight sub-series using MODWPT through the time based à trous filter algorithm [16]. Each subseries after being standardized is served as input to train a hybrid DL model. The latter DL architecture employs 1D-CNN layer with 128 filters of size 5. After convolution, the output is then transferred to LSTM layers with batch size 32. The optimizer employed was Adam and dropout layers with rate 0.2 were applied to prevent overfitting. Finally, the MLP layers consisted to 3 fully connected layers with 20, 10 and 5 neurons, respectively. Learning process took around 200 epochs to become stable. The outputs of each of the networks are then reconstructed to obtain a final solar irradiance prediction. Figure 1 shows the forecasting framework of MODWPT-CNN-LSTM-MLP.

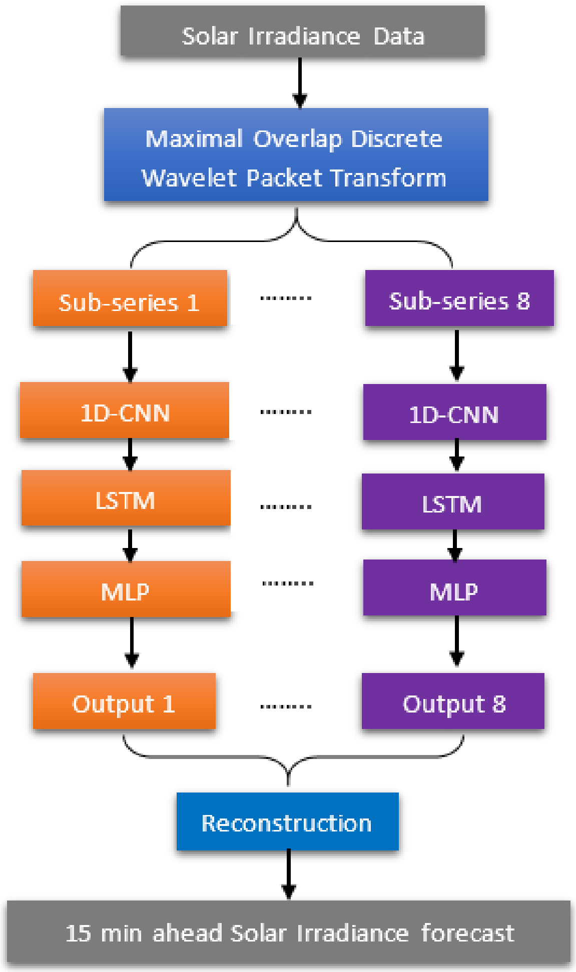

FIGURE 1. Forecasting framework of MODWPT-CNN-LSTM-MLP

Maximal Overlap Discrete Wavelet Packet Transform

WPT is a special variant of wavelet transform that refrains from discarding any high-frequency information, resulting in an improved and rigorous signal processing [17]. MODWPT is a special type of WPT which is non-decimated, thus ensuring that each level of decomposition retains the same number of wavelet coefficients. Additionally, MODWPT conserves energy of the signal. Equations (1), (2) and (3) are employed, where u represents the wavelet packet, h symbolize the low-pass filter, g represent the high-pass filter and $k \in Z$ being the depth. The algorithm for implementing MODWPT's is available in [18] and [19].

$$u_{2n}(t) = \sqrt{2} \sum_k h_k u(2t - k) \tag{1}$$

$$u_{2n+1}(t) = \sqrt{2} \sum_k g_k u(2t - k) \tag{2}$$

$$u_n = 2 \sum_k h(t - 2k) u_n(k) + 2 \sum_k g(t - 2k) u_{2n+1}(k) \tag{3}$$

1D-Convolutional Neural Network (1D-CNN)

The CNN consists of various layers and deals fundamentally with images as input. In this study a 1D-CNN is employed to deal with time series data. The first layer which is the 1D-convolutional layer which extract local feature from the input through a convolutional operation and subsequently applying a non-linear activation function to generate the output feature maps. Then a pooling layer is then employed for dimensionality reduction. Finally, a fully connected layer perform a non-linear mapping to produce the final output.

Long-Short Term Memory Neural Network (LSTM)

LSTM is a variant of the Recurrent Neural Network (RNN) which was designed to overcome the vanishing and exploding gradient problems [20]. This is achieved through a gating mechanism, comprising an input gate, a forget gate, and an output gate, which regulates the flow of data within a memory cell. This allows the LSTM to selectively retain key information over time, thereby effectively modeling long-range dependencies in temporal data while maintaining a constant error rate [21].

Multi-Layer Perceptron (MLP)

MLP is a feedforward artificial neural network consisting of one or more hidden layers. MLP is a strong tool that serves as a function approximator connecting the input and output, allowing non-linear modeling of complicated problems that are beyond the capacity of a single layer neural network. However, when increasing the number of nodes, the network will be more likely to overfit [22].

PERFORMANCE EVALUATION

Mean Absolute Error (MAE), Mean Bias Error (MBE), Root Mean Square Error (RMSE) and the coefficient of determination (R^2) are employed to evaluate performance of the models. These statistics measure the accuracy of the solar irradiance forecasts against the actual recorded data. With y being the actual irradiance data and $\hat{y}$ is the predicted irradiance, the metrics are computed as follows:

$$MAE = \frac{1}{N}\sum_{i=1}^{N}|y - \hat{y}| \tag{4}$$

$$MBE = \frac{1}{N}\sum_{i=1}^{N}(y - \hat{y}) \tag{5}$$

$$RMSE = \sqrt{\frac{1}{N}\sum_{i=1}^{N}(y - \hat{y})^2} \tag{6}$$

$$R^2 = 1 - \frac{\sum_{i=1}^{N}(y - \hat{y})^2}{\sum_{i=1}^{N}(y - \bar{y})^2} \tag{7}$$

ANALYSIS OF RESULTS

This section provides a detailed analysis of the performance of the three hybrid models namely, MODWPT-CNN-LSTM-MLP, MODWPT-LSTM-MLP, and MODWPT-LSTM for 15-minute-ahead solar irradiance forecasting. The analysis is conducted both on an overall basis and across different hourly intervals.

Table 1 displays the overall performance evaluation for the models. It can be seen that the MODWPT-CNN-LSTM-MLP show a superior performance, achieving the highest R^2 of 0.9989 along with the lowest MAE of 5.95, RMSE of 7.75, and an MBE close to zero at -1.66. This indicates that, on average, its forecasts are unbiased. Further, the second-best model is the MODWPT-LSTM-MLP, with significantly higher MAE of 9.98, RMSE of 12.78, R^2 of 0.9978 and an MBE of 3.69, which indicates an overestimation on average. Finally, the MODWPT-LSTM is the least accurate model with an MAE of 13.02, RMSE of 16.17, R^2 of 0.9975 and an MBE of -9.14, implying a strong underestimation of the irradiance. The plot illustrated in figure 2 evidences the superior forecasting performance of the MODWPT-CNN-LSTM-MLP as it accurately follows the true irradiance pattern compared to MODWPT-LSTM-MLP and MODWPT-CNN-LSTM models which consistently underestimates peak irradiance values.

TABLE 1. Performance Evaluation

Performance Metric	MODWPT-CNN-LSTM-MLP	MODWPT-LSTM-MLP	MODWPT-LSTM
MAE (W/m^2)	5.951063334	9.978115223	13.02104386
RMSE (W/m^2)	7.749654096	12.78287611	16.17027821
MBE (W/m^2)	-1.660809669	3.694430628	-9.139853482
R^2	0.9989	0.9978	0.9975

The MODWPT allows the separation of the various high and low frequencies within the solar irradiance time series, making training process easier for the networks. The advantage of a multi-level, hierarchical feature extraction process can be seen by the progressive improvement from MODWPT-LSTM to MODWPT-LSTM-MLP and finally to MODWPT-CNN-LSTM-MLP. The above also demonstrates that the inclusion of the 1D-CNN layers, significantly increase the accuracy of forecasts. The 1D-CNN layer effectively extracts local, high-frequency patterns from the MODWPT coefficients, creating a more refine and informative feature map for the LSTM. Without this 1D-CNN filter, the LSTM is burdened with less informative data, leading to higher bias and error as observed by the higher MAE and RMSE of MODWPT-LSTM to MODWPT-LSTM-MLP.

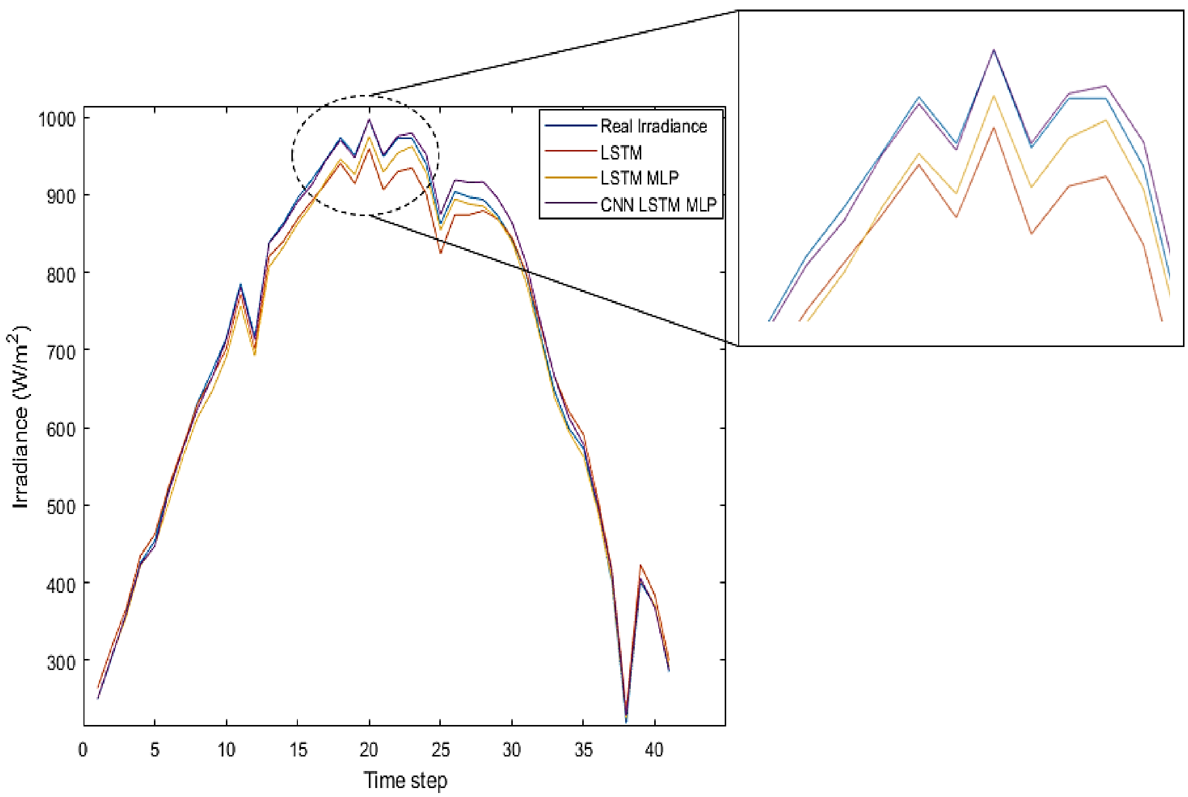

FIGURE 2. Performance on 8th Nov 2019

A granular analysis of the hourly performance shed light on the fluctuating forecast performances of all models throughout the day. Figure 3 illustrates the hourly performance analysis in terms of MAE, RMSE and MBE of the three models.

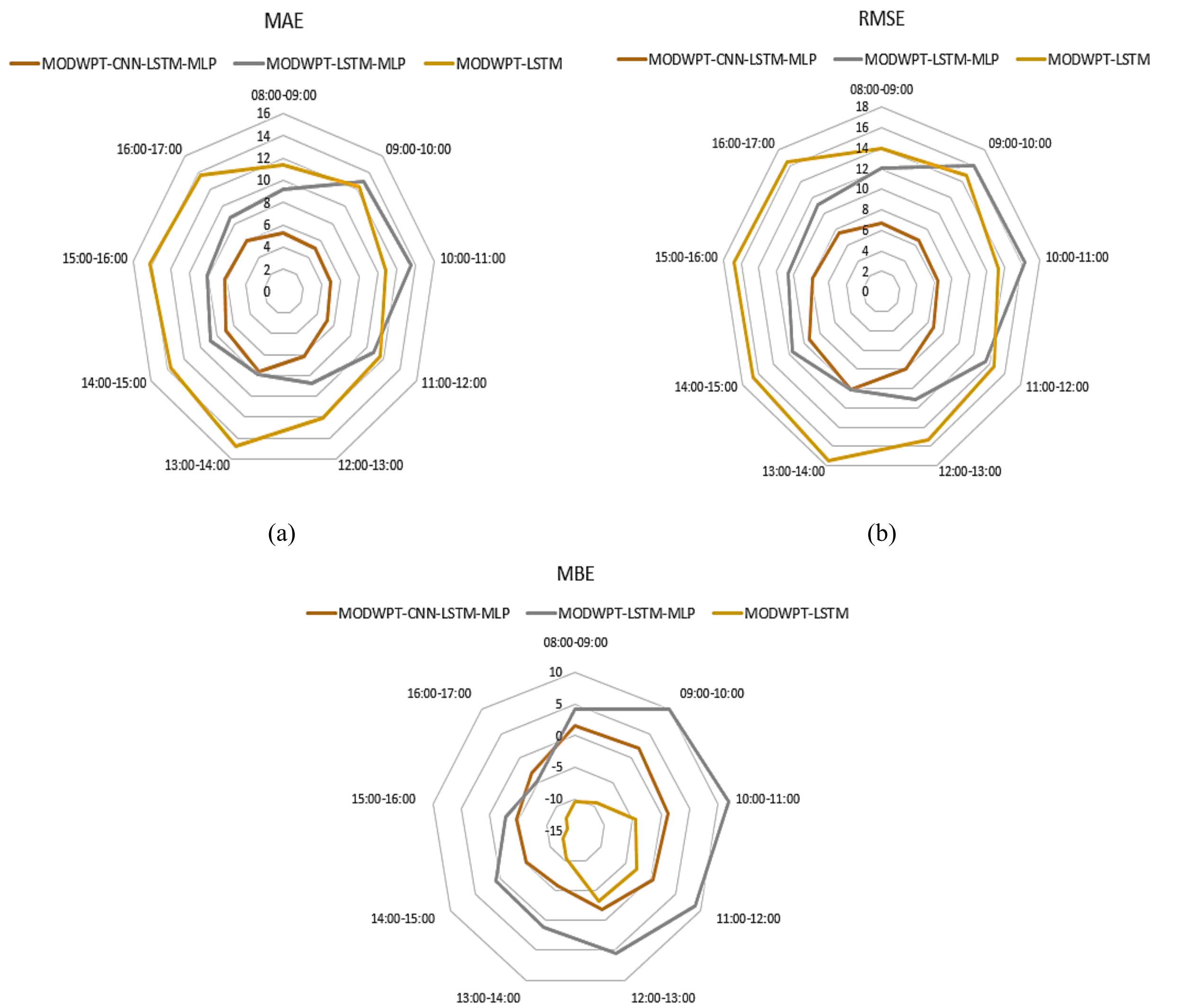

(a) (b)

(c)

FIGURE 3. Hourly performance analysis in terms of (a) MAE, (b) RMSE and (c) MBE of the three models

During the early morning till noon, solar irradiance rises until it becomes stable. This period showcases the best performance for all models, particularly for the MODWPT-CNN-LSTM-MLP model. The latter model's MAE remains lowest, ranging from 4.98 to 5.27, whilst its RMSE is below 6.79. The MBE of MODWPT-CNN-LSTM-MLP during this period of time is slightly positive, indicating on average a minor overestimation of irradiance. On the other hand, the MODWPT-LSTM-MLP model shows a significantly larger positive MBE, with values exceeding 10. This suggest the MLP layer in the latter model may be learning an overly aggressive rising trend, without the 1D CNN layer, causing it to overshoot the actual irradiance. Regarding the MODWPT-LSTM, a negative MBE is observed implying that the latter model consistently underestimates irradiance and is therefore unable to fully capture the increasing trend during this period of time.

From noon onwards, the tropical island of Mauritius faces increased atmospheric instabilities such cloud cover, convectional rain amongst others, inducing higher solar heterogeneity. Even the MODWPT-CNN-LSTM-MLP model experiences a slight drop forecasting performance, with its MAE and RMSE peaking around 13:00-14:00. It can be also noted through the MBE that the model slightly underestimates irradiance when cloud cover, convectional rain or other transient phenomena occur. Even though, MODWPT-CNN-LSTM-MLP shows a slight drop in performance, its forecast errors are substantially lower than the other two models, demonstrating its robustness to volatility. This is due to the ability of the CNN in identifying the localized, high-frequency signatures in the wavelet data corresponding to cloud passage. In contrast, the MODWPT-LSTM-MLP model shows an increase in performance with lower MAE and RMSE decrease and an MBE approaching zero compared to the forenoon. However, it fails to effectively capture critical dynamics as the CNN-based model, as evidenced by its higher MAE and RMSE. The performance of the MODWPT-LSTM model deteriorates further when faced with volatile data during the afternoon. It shows the highest MAE and RMSE and a strong negative MBE. The latter network fails to predict irradiance fluctuation caused by cloud cover amongst others. This suggests that the LSTM alone struggles with the high-frequency components, even after wavelet decomposition.

CONCLUSION

In this paper, three hybrid models namely the MODWPT-CNN-LSTM-MLP, MODWPT-LSTM-MLP and the MODWPT-LSTM are developed for the 15 minutes ahead solar irradiance forecasting. The key contributions of the present research are summarized below. The MODWPT-CNN-LSTM-MLP outperforms all the other models with lowest values of MAE, RMSE, R^2 and an MBE close to zero. A progressive improvement of a multi-level, hierarchical feature extraction process can be observed from MODWPT-LSTM to MODWPT-LSTM-MLP and finally to MODWPT-CNN-LSTM-MLP. All models employ LSTM which is essential for modeling time dependencies. Nevertheless, its effectiveness is dependent on the quality of the input features it receives. Hence the inclusion of the 1D-CNN layers which extract patterns from the MODWPT coefficients, creating a more refine and informative feature map for the LSTM. Networks without the 1D-CNN filter, like the MODWPT-LSTM and MODWPT-LSTM-MLP yield in higher MAE and RMSE values. A granular analysis of the hourly performance revealed that during the forenoon, all models showed their best performance, especially the MODWPT-CNN-LSTM-MLP with the lowest MAE ranging from 4.98 to 5.27, whilst its RMSE is below 6.79. However, during the afternoon session coincides with peak solar heating, which often triggers convectional rain and cloud formation, resulting in solar irradiance variability. The latter variability slightly impacts the performance of the MODWPT-CNN-LSTM-MLP as seen on the rise in MAE and RMSE values. Surprisingly, the MODWPT-LSTM-MLP network showed some adaption to this afternoon variability with lower MAE and RMSE, though not as effectively as the CNN-based model.

This paper presents an accurate hybrid solar irradiance forecasting model namely the MODWPT-CNN-LSTM-MLP which can help reduce the impact of the intermittent nature of solar energy and therefore improves the stability and reliability of the PV system. The proposed model can help increases the penetration level of the PV system and to promote the integration of PV power into power grids. Future studies can be geared towards the performance evaluation of the proposed model for longer forecasting horizons and a comparison to other class of forecasters like the statistical Johansen VECM and other empirical models.

ACKNOWLEDGMENTS

This work has been conducted under the HEC (Higher Education Commission Mauritius) MPhil/PhD scholarship. The authors wish to thank Miss Rawsiya Khadaroo for her help and support.

REFERENCES

1. S. Sobri, S. Koohi-Kamali, and N. A. Rahim, *Energy Convers. Manage.* **156**, 459 (2018).
2. M. Pushpavalli, D. Dhanya, M. Kulkarni, R. J. Jasmine, B. Umarani, M. RamprasadReddy, and A. Rajaram, *Electr. Power Compon. Syst.* **52**, 1 (2024).
3. P. Kumari and D. Toshniwal, *J. Clean. Prod.* **318**, 128566 (2021).
4. E. Chodakowska, J. Nazarko, Ł. Nazarko, and H. S. Rabayah, *Energies* **17**, 3156 (2024).
5. A. E. Gürel, Ü. Ağbulut, H. Bakır, A. Ergün, and G. Yıldız, *Heliyon* **9**, e13214 (2023).
6. C. M. Travieso-González, F. Cabrera-Quintero, A. Pinan-Roescher, and S. Celada-Bernal, *Appl. Sci.* **14**, 5605 (2024).
7. L. Nonnenmacher and C. F. M. Coimbra, *Sol. Energy* **108**, 447 (2014).
8. Occhipinti, G., "Impacts of stochastic fluctuations on marine biogeochemical processes," Ph.D. thesis, University of Trieste, (2024).
9. Z. Coya, A. Khoodaruth, H. Ramenah, V. Oree, A. P. Murdan, and M. Bessafi, "Comparing the Johansen VECM model to an AI hybrid model for the short term photovoltaic power forecasting," in *1st International Conference on Smart Energy Systems and Artificial Intelligence (SESAI)* (IEEE, 2024) pp. 1–6.
10. O. O. Apeh and N. I. Nwulu, *J. Environ. Earth Sci.* **7**, (2025).

11. M. Khodayar, J. Wang, and M. Manthouri, *IEEE Trans. Smart Grid* **10**, 3974 (2018).
12. W. Ye, G. Zheng, X. Cao, Y. Ma, and A. Zhang, arXiv:2402.12715 (2024).
13. H. Wang, Z. Lei, X. Zhang, B. Zhou, and J. Peng, *Energy Convers. Manage.* **198**, 111799 (2019).
14. K. Kawaguchi, Y. Bengio, and L. P. Kaelbling, "Generalization in deep learning," in *Mathematical Aspects of Deep Learning*, edited by P. Grohs (Cambridge University Press, United Kingdom, 2022) pp. 112–148.
15. Z. Coya, A. Khoodaruth, H. Ramenah, V. Oree, A. P. Murdan, and M. Bessafi, "Deep learning models in photovoltaic power forecasting: a review," in *1st International Conference on Smart Energy Systems and Artificial Intelligence (SESAI)* (IEEE, 2024) pp. 1–9.
16. B. L. Zhang, R. Coggins, M. A. Jabri, D. Dersch, and B. Flower, *IEEE Trans. Neural Netw.* **12**, 765 (2001).
17. A. Hussain, T. A. M. Janjua, A. N. Malik, A. Najib, and S. A. Khan, *Mech. Syst. Signal Process.* **212**, 111326 (2024).
18. A. T. Walden and A. C. Cristan, *Proc. R. Soc. London, Ser. A* **454**, 2243 (1998).
19. D. B. Percival and A. T. Walden, *Wavelet Methods for Time Series Analysis Vol. 4* (Cambridge University Press, Cambridge, 2000).
20. I. D. Mienye, T. G. Swart, and G. Obaido, *Information* **15**, 517 (2024).
21. S. Hochreiter, Y. Bengio, P. Frasconi, and J. Schmidhuber, "Gradient flow in recurrent nets: the difficulty of learning long-term dependencies," in *A Field Guide to Dynamical Recurrent Networks*, edited by J. F. Kolen and S. C. Kremer (Wiley-IEEE, 2001) pp. 237–243.
22. D. T. Bui, V. H. Nhu, and N. D. Hoang, *Adv. Eng. Inform.* **38**, 593 (2018).